Sule Lamido University Journal of Science & Technology Vol. 5 No. 1&2 [Dec, 2022], pp. 41-49
https://doi.org/10.56471/slujst.v5i.253

Online ISSN: 2736-0903
Print ISSN: 2736-089X
www.slujst.edu.ng

Adsorptive Potency of Activated Carbonized Avocado Pear Seeds (*Persea Americana)* and Activated Carbonized orange peels (*Citrus Sinensis*) in Eliminating Pb^{2+} ions in Contaminated Water

Okponmwense Moses[1*] and Alfred David Chukwuemeka[2]
[1,2]Department of Chemistry, Faculty of Physical Sciences, University of Benin, Benin City. Nigeria
*Corresponding author: okponmwense.moses@uniben.edu

Abstract

***Background**: Heavy metals persistence in water brings about undesirable effect on man and animal because they are not degradable like other organic pollutants. **Aim:** The research work seek to examine adsorptive effectiveness of activated carbonized avocado pear seed as well as Activated Carbonized orange peels in getting rid of Pb^{2+} ions from contaminated water. **Method**: Carbonized Avocado Pear seed (CAPS) as well as carbonized orange peel (COP) was impregnated with Potassium hydroxide (KOH) in ratio 1:1 for 48 hours. The impregnated KOH CAPS and COP was separately washed and oven dried at 105℃ for 6 hours and thereafter heated in a muffle furnace (Carbolite AAF1100) at 250^0C for 1 hour. The activated carbonized pear seed (ACAPS) and activated carbonized orange peel (ACOP) obtained was physicochemically described using SEM and FTIR. The adsorption route of Pb^{2+} ion on top of ACAPS as well as ACOP was examined by means of batch adsorption isotherm investigation. The Pb^{2+} ion adsorption pattern was assessed with Langmuir, DRK, Freundlich, Tempkin and Flory-Huggin isotherm models. **Results**: The SEM photograph, disclosed that ACAPS posessed numerous openings of different dimensions whereas ACOP possessed less openings of lesser dimensions. R^2 worth ranging from 0.92 to 1.00 was got, indicating that the whole isotherm models were capable of elucidating the connection in the figures obtained. The Pb^{2+} ion had a firmer attraction and adsorption capacity for ACAPS. Overall, ACAPS was a superior adsorbent likened with ACOP for effectual elimination of Pb^{2+} ion owing to a blend of its numerous pores of different dimensions and it surface functional groups with a q_m worth of 23.10 and 6.06mg/g in that order.*

Keywords: *Avocado, Orange, Physiosorption, Potency, Adsorptive.*

1. Introduction

There are heavy metals of various forms in the atmosphere, soil and the water bodies on earth. Heavy metals persist in the environment and unlike organic pollutants, they cannot be degraded hence triggering unfavorable consequence on man and animals. (Fu & Wang, 2011; Rasheed *et al*., 2013; Kumar *et al*., 2014). The major users of lead are batteries storage industry and petroleum industry in manufacturing gasoline additives. However, lead ions are obtained from television tube, paint, printing, pigments, photographic materials, fuels, matches, automobile emission, mining and explosives. Lead is poisonous to nearly all living things. It was known to cause harm to vital human organs such as the lungs, kidney, liver, reproductive system, brain and basic cellular processes. Soaring knowledge of the ecological effect of lead (Pb^{2+}) ions has provoked calls for decontamination of polluted water preceding release into waters bodies (Lakherwal, 2014; Singh & Gupta, 2016 and Abdel-Raouf & Abdul-Raheim, 2017).

Owing to the degree of problems of Pb^{2+} ion contamination, study into recent, effectual and cheap means of Pb^{2+} ion elimination is growing. Many literatures have pointed at the possible usage of agricultural wastes as suitable adsorbent for eliminating Pb^{2+} ion from contaminated waters. Contaminated water treatment with agricultural waste adsorbent is extra cost effectual compared to usage of established adsorbents such as commercial activated carbon (Abia and Igwe, 2005). Many means for eliminating heavy metal ions from contaminated water exist, based on physical, chemical and biological mechanisms (Miretzky *et al*., 2006), likewise, many methods of contaminated water remedy like coagulation, chemical precipitation, ion exchange, sedimentation, adsorption, disinfection, ultra-filtration, nano-filtration, and reverse osmosis are in existence (Hossain *et al*., 2012; Kumar *et al*., 2014), among these, adsorption procedure is by and large an efficient as

Sule Lamido University Journal of Science & Technology Vol. 5 No. 1&2 [Dec, 2022], pp. 41-49
https://doi.org/10.56471/slujst.v5i.253
Online ISSN: 2736-0903
Print ISSN: 2736-089X
www.slujst.edu.ng

well as cost-effective process for contaminated water remediation because of its suitability, stress-free procedure and ease of construct (Kampalanonwat and Supaphol, 2014, Abdel-Raouf and Abdul-Raheim, 2017**)**. The research work seek to examine adsorptive effectiveness of activated carbonized avocado pear seed as well as Activated Carbonized orange peels in getting rid of Pb^{2+} ions from contaminated water.

2. Materials and Methodologies

2.1. Samples collection

The orange peel and Avocado seed were purchased from New-Benin market in Benin City, Nigeria. The peel and seed of the orange and Avacado respectively, were separated from the fruit, cut into smaller pieces and reduced dimensions. Thereafter, were rinsed using distilled water to eliminate dirt and dried under sun for 6 days. The dried materials were transferred separately into a sealed polyethylene bag for upward analysis.

2.2. Preparation of activated carbonized avocado pear seed (ACAPS) and activated carbonized orange peels (ACOP)

The dried up avocado pear seed was pulverized into powder appearance and sifted by means of standard test sieve (BSS-53 µm mesh sieve), similarly, the orange peel was treated in like manner. Each of them was separately carbonized in a muffle furnace (Carbolite AAF1100) at 300^0C for 40 minutes. The carbonized avocado pear seed and carbonized orange peel was soaked with potassium hydroxide (KOH) using a soaking ratio of 1:1 for 48 hours till the mix turned into a paste in different containers. This was done to increase the surface area and perviousness of the activated carbon. KOH is a strong dehydrating agent as well as modifies the carbon to form porous structure, this makes it the desired activating agent. The ACAPS and ACOP were rinsed individually applying distilled water till the pH of the filtrate was 7. The ACAPS and ACOP was oven dried at 105℃ for 6 hours and reheated in a muffle furnace (Carbolite AAF1100) at 250^0C for 1 hour.

2.3. Adsorbates preparation and characterization

Simulated Pb^{2+} ions contaminated water was prepared with lead nitrate salt of analytical grade from BDH. The definite concentrations were verified with atomic absorption spectrophotometer (AAS).

2.4. Physicochemical characterization of activated carbonized avocado pear seed (ACAPS) and activated carbonized orange peels (ACOP)

The physicochemical description of ACAPS as well as ACOP was sorted out employing scanning electron microscope (phenom pro suite desktop - SEM) was used for imageries which reveals their morphologies, Fourier transform infrared (FTIR) spectrophotometer was employed in ascertaining functional groups display.

2.5. Adsorption Isotherm Studies

The adsorption route of Pb^{2+} ions on top of ACAPS as well as ACOP was investigated, applying the batch adsorption isotherm experiment and consequences of adsorbent amounts, interaction period, pH and initial concentration on the elimination of Pb^{2+} ion were examined. The batch adsorption experiment was performed by differing adsorbent amount from 0.2g to 2.5g, interaction period from 20 min. to 100 min. and pH from 3 to 7 at unvarying Pb^{2+} ions concentration. Initial concentration of Pb^{2+} ion was differed from 20 mg/L to 100 mg/L, at optimal adsorbent dosages, interaction period, pH as well as shakeup speediness of 300 rpm. The Pb^{2+} ion equilibrium concentration in the treated water was established by means of AAS (Buck scientific model VGP-210).

2.6. Theory: Adsorption Mechanism and Adsorption Isotherm

Classically, adsorption mechanisms include adsorbate diffusion onto adsorbent surface by intermolecular forces in the middle of adsorbate and the adsorbent superficial; adsorbate migrating into adsorbent openings and adsorbate one-tracklayer accumulation on the adsorbent (Iakovleva and Sillanpää, 2013). Nevertheless, the prime means for heavy metal ions (M^{2+}) removal, could be ion exchange, owing to existence functional groups diversities atop adsorbents superficial for instance hydroxyl, carboxylic, carbonyl e.t.c, (He *et al.*, 2019).

The equilibrium quantity of adsorbate adsorbed as well as adsorption effectiveness in the contaminated water were estimated with the use of equation 1 and 2 in that order:

Sule Lamido University Journal of Science & Technology Vol. 5 No. 1&2 [Dec, 2022], pp. 41-49
https://doi.org/10.56471/slujst.v5i.253
Online ISSN: 2736-0903
Print ISSN: 2736-089X
www.slujst.edu.ng

$$q_e = \frac{(C_o - C_e)v}{M} \quad (1)$$

$$\%E = \frac{C_o - C_e}{C_o} \times 100 \quad (2)$$

The parameters C_0 is the adsorbate's initial concentration (mg/L); q_e and C_e are the Cd^{2+} ions quantity adsorbed (mg/g) as well as adsorbate equilibrium concentration (mg/L), in that order; M is adsorbent weight (g) and v is aqueous solution amount in litres.

Isotherm models of Langmuir, Freundlich, Dubinin–Radushkevich, Tempkin and Flory-Huggin were utilized to appraise obtained data in this study. Langmuir isotherm model is based on detail that one-tracklayer adsorption exist, happening homogeneously on the adsorbent operational locations and absence of exchanges amid the adsorbates. It is mainly regularly utilized to evaluate the adsorbate quantity atop an adsorbent as a function of concentration in a specified temperature (Almalike, 2017; He *et al.*, 2019). Langmuir isotherm equation is shown in equation 3:

$$\frac{1}{q_e} = \frac{1}{q_m} + \frac{1}{K_l q_m C_e} \quad (3)$$ (Ghasemi *et al.*, 2018, Lim *et al.*, 2019)

q_m is the speculative all-out one-tracklayer adsorption capacity (mg/g), and K_L (Lg^{-1}) denotes the Langmuir isotherm constant for adsorption energy.

Freundlich Isotherm model is worthwhile for non-ideal and multilayer adsorption route atop dissimilar surfaces with a non-uniform allocation of the adsorption heat on top of the surfaces (Iakovleva and Sillanpää, 2013; Lasheen *et al.*, 2017). The Freundlich isotherm equation is shown in equation 4:

$$\log q_e = \log k_F + (1/n_F)\log C_e \quad (4)$$ (Bankole *et al.*, 2019, Lim *et al.*, 2019)

The K_F and n_F remain the constants of Freundlich isotherm for adsorption capacity and strength, in that order. $1/n_F$ is a dimensionless heterogeneousness factor; it's worth point to which of the adsorption route is spontaneous. When n_F value is greater than 1, spontaneous adsorption conditions apply. The lesser the value of $1/n_F$, the more the heterogeneousness (Yildiz, 2017).

Dubinin–Radushkevich is a semi-empirical equation predicated upon micropores volume fill up principle (MVFP) (Worch, 2012), its adsorption mechanism keep an eye on a mechanism of pore filling (Sarı and Tuzen, 2009), it gives a consideration into adsorbent porousness as well as adsorption apparent free energy that offer facts on the adsorption route or adsorption mechanism nature, occurring on either homogeneous and heterogeneous surfaces that is, whether chemisorption or physisorption (Essomba *et al.*, 2014; Inyinbor *et al.*, 2015; Onwu & Ngele, 2015). Isotherm model of Dubinin–Radushkevich is unfounded on ideal assumptions for instance, steric encumbrance nonexistence in the middle of adsorbed and entering particles, equal efficacy of the adsorption locations and surface uniformity on microscopic level as in Langmuir isotherm (Sarı and Tuzen, 2009; Amin *et al.*, 2015; Moftakhar *et al.*, 2016). The Dubinin–Radushkevich equation (equation 5) has been broadly applied to expound energetic heterogeneousness of solid at low level coverage as one-tracklayer zones in micropores (Hossain *et al.*, 2016; Inyinbor *et al.*, 2016). Dubinin–Radushkevich isotherm is regularly applied to illustrate solo solute systems adsorption isotherms (Essomba *et al.*, 2014).

$$\ln q_e = \ln q_D - \beta.\varepsilon^2 \quad (5)$$ (Adekola *et al.*, 2016, Ghasemi *et al.*, 2018)

$$[\varepsilon = RT\ln(1+1/C_e)] \quad (5a)$$

$$E = 1/(-2\beta)^{1/2} \quad (5b)$$

q_D (mol/g) signifies all-out adsorption capacity, β is the constant of Dubinin–Radushkevich isotherm (mol^2/kJ^2), it denotes adsorbate free energy per mole as the aforementioned rove to the surface of the adsorbent from inestimable distance. E is adsorption mean free energy (kJ/mol), if E is less than 8, the adsorption means is governed by physisorption route, if E is greater than or equal to 8 or E is less than or equal to 16, then adsorption route is governed via chemisorption (ion-exchange route) route as well as if E is greater than 16, the adsorption means is governed via diffusion of particle. Gas constant, R = 8.314 J/molK, absolute temperature represented as T in Kelvin and ε is Polanyi (adsorption) potential energy.

The Temkin isotherm model was based on chemisorptions notion as well as adopts that the adsorption heat of adsorbate molecules reduces linearly by means of adsorbent layer coverage owing to adsorbent-adsorbate exchanges, it similarly adopts a uniform binding energies allocation (Tie *et al.*, 2017). The Temkin isotherm equation is shown in equation 6:

$$q_e = B\ln K_T + B\ln C_e \quad (6)$$ (Tie *et al.*, 2017)

$$B = (RT/b_T) \quad (6a)$$

Sule Lamido University Journal of Science & Technology Vol. 5 No. 1&2 [Dec, 2022], pp. 41-49
https://doi.org/10.56471/slujst.v5i.253
Online ISSN: 2736-0903
Print ISSN: 2736-089X
www.slujst.edu.ng

B is heat of adsoption (B = RT/b_T); b_T (J/mol), is the Temkin isotherm constant; K_T (L/g), is equilibrium binding constant as well as linked to all-out binding energy (Tie *et al.*, 2017, Ghasemi *et al.*, 2018, Bankole *et al.*, 2019).

Flory-Huggins isotherm is useful in describing the degree of surface coverage appearances of the adsorbate on the adsorbent, This isotherm model can state the possibility and spontaneity of an adsorption route (Almalike, 2017, Ayawei *et al.*, 2017). The Flory-Huggins isotherm equation is shown in equation 7:

Log (θ/C_o) = Log K_{FH} + n_{FH} Log (1−θ) (Flory-Huggins isotherm) (7) (Almalike, 2017, Ayawei *et al.*, 2017)

[θ = (1- [C_e/C_0])] (7a)

ΔG^o = -RTlnk_{FH} (7b)

θ is the surface coverage of the adsorbent by the adsorbate, C_o is initial concentrations, K_{FH} and n_{FH} are Flory-Huggins model equilibrium constant and n_{FH} is the number of adsorbate dwelling in adsorption site respectively. ΔG^o is standard free energy change. If the ΔG^o calculated is negative, it implies adsorption route was spontaneous in nature as well as supports an exothermic nature and vice versa if positive (Almalike, 2017).

On the whole, the isotherm factors are principally calculated from their linear plots intercept and slope. Isotherm models fitting were evaluated using R^2 values.

3. Results

3.1. Characterization for activated carbonized avocado pear seed (ACAPS) and activated carbonized orange peels (ACOP)

The ACAPS as well as ACOP was characterised by means of SEM and FTIR. The ensuing characteristics descriptions were found:

3.1.1. Scanning electron microscopy (SEM) analysis

SEM imageries (Fig. 1a and 1b), reveals the surface morphology of ACAPS as well as ACOP.

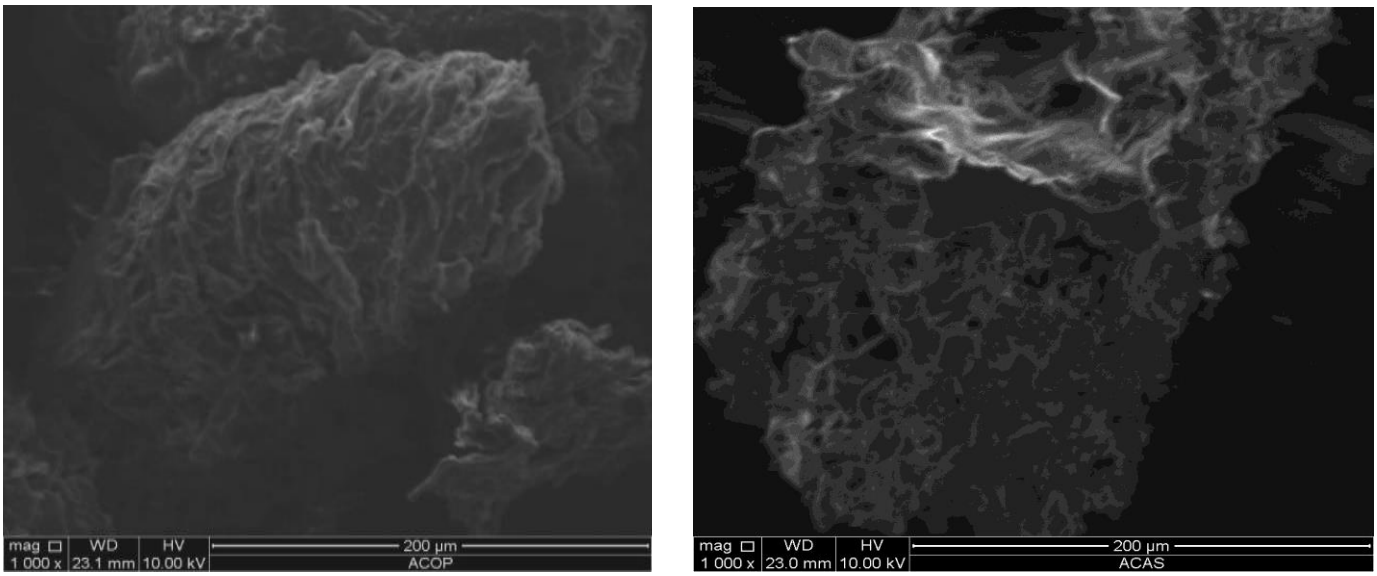

(1a) (1b)

Figure 1: SEM images of ACOP (1a) and ACAPS (1b) (at 1000X magnification)

3.1.2 Fourier transformed infrared spectroscopy (FTIR) analysis

FTIR analysis spectrum (Fig. 2), showing the functional groups existing on ACOP and ACAPS.

Sule Lamido University Journal of Science & Technology Vol. 5 No. 1&2 [Dec, 2022], pp. 41-49
https://doi.org/10.56471/slujst.v5i.253
Online ISSN: 2736-0903
Print ISSN: 2736-089X
www.slujst.edu.ng

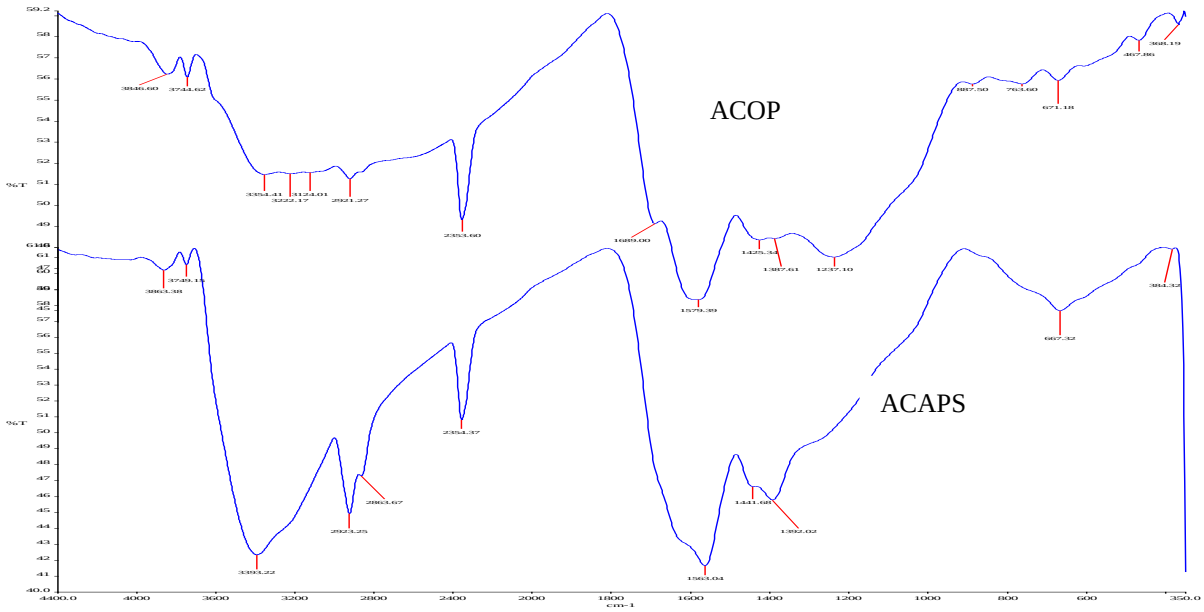

Figure 2: FTIR Spectrum for ACOP and ACAPS

3.2. Isothermal models for lead ion adsorption

Isothermal models for the adsorption prototype of Pb^{2+} ion atop ACAPS and ACOP are revealed in Fig. 3 (a-e).

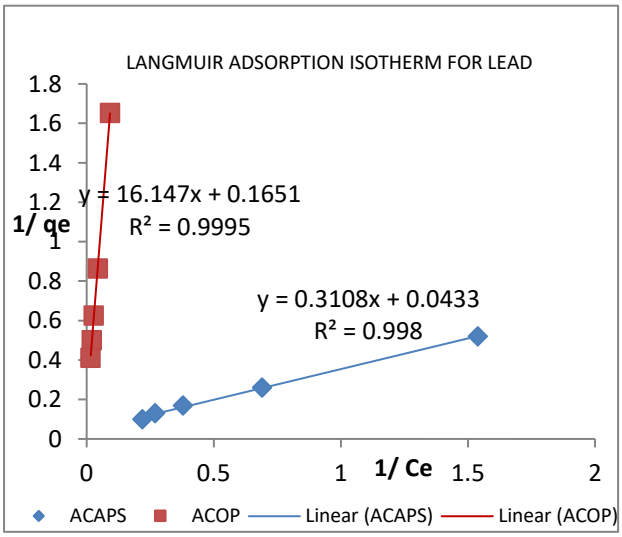

(3a)

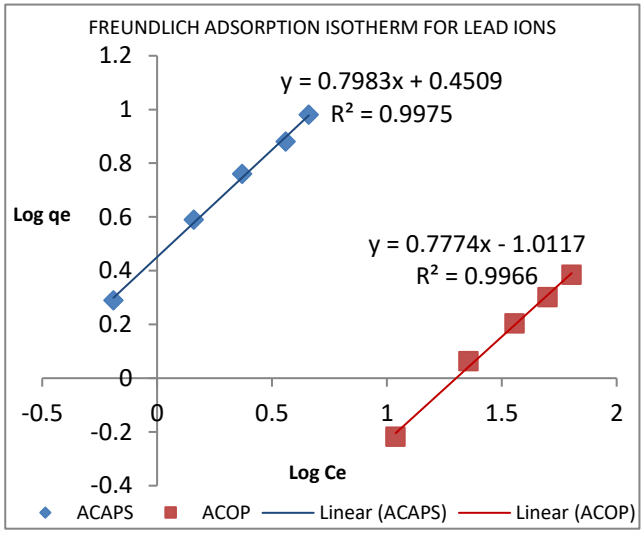

(3b)

Fig 3: graphical illustration of isothermal models for Pb^{2+} ion adsorption (a-b)

Sule Lamido University Journal of Science & Technology Vol. 5 No. 1&2 [Dec, 2022], pp. 41-49
https://doi.org/10.56471/slujst.v5i.253
Online ISSN: 2736-0903
Print ISSN: 2736-089X
www.slujst.edu.ng

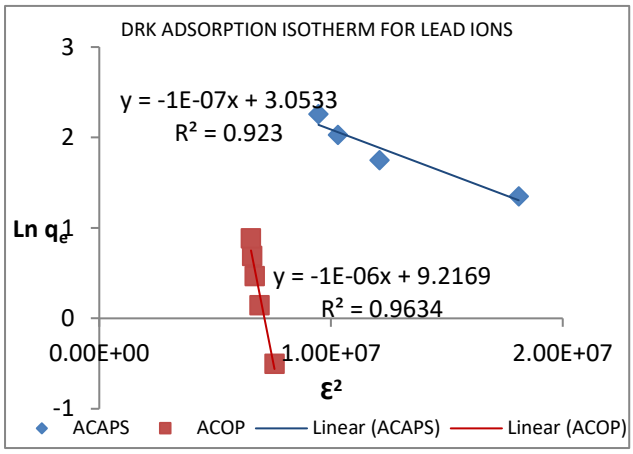

(3c)

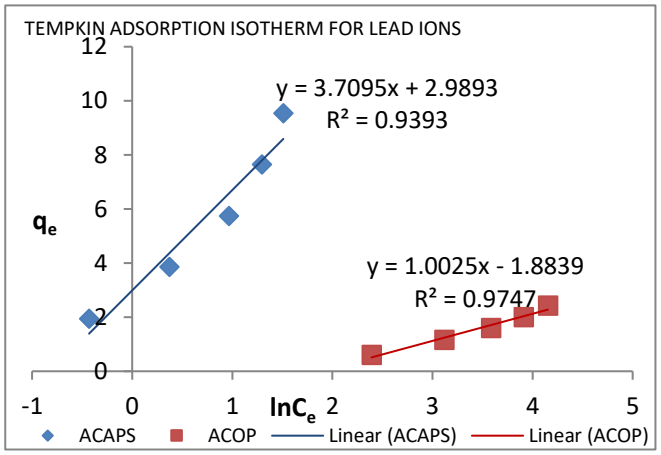

(3d)

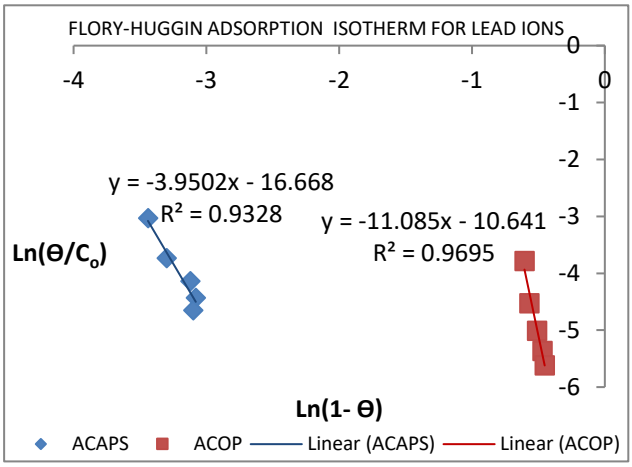

(3e)

Fig 3: graphical illustration of isothermal models for Pb^{2+} ion adsorption (c-e)

Table 1: Adsorption isotherm model parameters

Adsorption Isotherm Model	**Parameters**	**Units**	**ACOP**	**ACAPS**
Langmuir	R^2	-	1.00	1.00
$1/q_e = 1/q_m + 1/K_L q_m C_e$	k_L	l/g	0.01	0.139
	q_m	mg/g	6.06	23.10
Freundlich	R^2	-	1.00	1.00
$\log q_e = \log k_f + (1/n_f)\log C_e$	K_F	-	0.10	2.82
	n_F	-	1.29	1.25
Dubinin-Radushkevick (DRK)	R^2	-	0.96	0.92
$\ln q_e = \ln q_m - \beta.\varepsilon^2$	q_D	mg/g	10065.81	21.19
$[\varepsilon = RT\ln(1+1/C_e)]$	B	J/molecule	1.0×10^{-6}	1.0×10^{-7}
	E	kJ/mol	0.707	2.24
Tempkin	R^2	-	0.97	0.94
$q_e = B \ln K_T + B \ln C_e$	K_T	l/g	0.15	2.24
$B = (RT/b_T)$	b_T	J/mol	2.5×10^3	6.79×10^2
	B	-	1.00	3.71
Flory-Huggins	R^2	-	0.97	0.93
$\text{Log}\ (\theta/C_o) = \text{Log}\ K_{FH} + n\ \text{Log}\ (1-\theta)$	K_{FH}	$Lmol^{-1}$	2.29×10^{-11}	2.15×10^{-17}
$[\theta = (1- [C_e/C_0])]$	n_{FH}	-	11.09	3.95
	ΔG^o	J	-5.77×10^{-8}	-5.42×10^{-14}

Online ISSN: 2736-0903
Print ISSN: 2736-089X
www.slujst.edu.ng

4. Discussion

4.1. Characterization of activated carbonized avocado pear seed (ACAPS) and activated carbonized orange peels (ACOP)

The SEM imageries (Fig. 1), revealed that activated carbonized avocado pear seed posesses wide variety of pores along with fibrous structure while the activated carbonized orange peel had smaller amount pores of lesser sizes. The SEM images of both adsorbent revealed that the particles are made up of pores possessing uneven shapes. The fragmention of the particles and variance in opening dimension portrays the variances in physical appearances concerning ACOP as well as ACAPS.

The FTIR spectrum for ACAPS (Fig. 2) revealed the descriptions of a very strong band at 3393.15cm^{-1} which characterized medium appearance of NH-stretching vibrations of primary amine RNH_2 as well as secondary amine R_2NH group. Similarly, peak at 2923.25cm^{-1} agreed to OH-stretch of carboxylic acids (-COOH) group. The peak at 1580.61 agreed to a medium appearance of firm –C-H stretch of alkyl group of CH_3 an electron donating moiety (with positive inductive effect) that can boost the adsorption of Pb^{2+}. Also, a peak at 1441.68cm^{-1} agreed to a firm C-H bend allocated to alkyl group. The FTIR spectrum of ACOP (Fig. 2) showed attribute peak at 3354.41 and 3124.01 agreeing to a medium N-H stretch of primary as well as secondary amines group and O-H stretch (H-bonded) of carboxylic acids (-COOH) in that order. The peak at 2921.27 and 1425.34cm^{-3} corresponded to a medium appearance of strong –C-H stretch and –C-H bend respectively of alkyl group of CH_3 an electron donating moiety (with positive inductive effect) that can boost the adsorption of Pb^{2+}. The peak at 1689.00 gave a very strong C=O stretch for amides ($RCONH_2$). A peak at 1237.10cm^{-3} revealed a firm –C-O stretch corresponding to acid, ester and anhydride (-COOH, RCOOR and $R(COOH)_2$).

4.2. Parameters from adsorption isotherm models for lead ion adsorption

The R^2 evaluation varied from 0.92 to 1.00, indicating that the whole isotherm models were capable to articulate the correlation in figures got (Table 1). The Langmuir and Freundlich isotherm constants showed that ACAPS had a firmer affinity and adsorption capacity than ACOP for Pb^{2+} ion grounded on their k_L and k_F (Table 1). However, ACOP had higher adsorption intensity than ACAPS for Pb^{2+} ion based on n_F values (Table 1). These observations are attributed to the various functional groups on the adsorption location on the adsorbents (Fig. 2). ACAPS adsorb more Pb^{2+} ions likened to ACOP established on the worth of their all-out adsorption capacity q_m from Langmuir isotherm model (Table 1), this was attributed to a blend of the functional groups and sizeable openings of different dimensions ACAPS possessed (Fig. 1). The Freundlich isotherm model likewise affirmed that the ACOP as well as ACAPS adsorbent adsorbed Pb^{2+} ions spontaneously as both adsorbent had an n_F worth more than 1 and the values of ΔG^o from the Flory-Huggins model confirmed that the adsorption route was spontaneous as well as exothermic (Table 1). Dubinin-Radushkeviek isotherm model's mean free energy of adsorption (E, kJ/mol) disclosed that adsorption means was governed via physiosorption route. The energy per mole (β) required by Pb^{2+} to migrate to ACOP surface is higher compared to that of ACAPS surface, this is in agreement with the adsorption intensity (n_F) of Pb^{2+} ions onto ACOP. Tempkin adsorption isotherm disclosed that ACAPS had a superior heat of adsoption (B) while ACOP had a higher maximum binding energy (k_T) (Table 1). The n_{FH} values for ACAPS and ACOP of 3.95 and 11.09 revealed that the ACAP had more adsorption site, However, ACOP takes up more Pb^{2+} ion per adsorption site as revealed Flory-huggins isotherm model n_{FH} values vis-a-vis Langmuir isotherm model q_m values.

5. Conclusions

The adsorption of Pb^{2+} ions onto ACOP and ACAPS was spontaneous, exothermic and occurred through a physiosorption mechanism. The affinity as well as adsorption capacity of ACAPS for Pb^{2+} ion was firmer likened to ACOP owing to functional group location atop its surface. Tempkin adsorption isotherm showed that ACAPS had a superior heat of adsorption (B) and maximum binding energy (k_T), indicating that the ACAPS had a stronger hold of Pb^{2+} ion atop its surface likened to that of ACOP. ACOP had higher adsorption intensity (n_F) for Pb^{2+} ion and this was corroborated by the fact that the Pb^{2+} ion migrate onto the ACOP

Online ISSN: 2736-0903
Print ISSN: 2736-089X
www.slujst.edu.ng

surface at a higher energy per mole (β). On the whole, activated carbonized avocado pear was a superior adsorbent likened with activated carbonized orange peel for effectual exclusion of Pb^{2+} ions from the contaminated water owing to a blend of its numerous pores of different dimensions and it surface functional groups.

References

Abdel-Raouf, M. S. and Abdul-Raheim, A. R. M (2017). Removal of Heavy Metals from Industrial Waste Water by Biomass-Based Materials: A Review. *Journal of Pollution Effects and Control* **5**(1)

Adekola, F. A., Adegoke, H. I. and Ajikanle, R. A. (2016). Kinetic and Equilibrium Studies of Pb(II) And Cd(II) Adsorption On African Wild Mango (*Irvingia Gabonensis*) Shell. *Bulletin Chemical Society of Ethiopia* 30(2):185-198.

Almalike, L. B. (2017). Equations Adsorption Isotherms for Biuret on Soils, Paper and Cortex Plant Application of the Freundlich, Langmuir, Temkin, Elovich, Flory-Huggins, Halsey and Harkins-Jura. *International Journal of Advanced Research in Chemical Science* 4(5):9-20.

Amin, M. T., Alazba, A. A. and Shafiq, M.(2015). Adsorptive Removal of Reactive Black 5 from Wastewater Using Bentonite Clay: Isotherms, Kinetics and Thermodynamics. *Sustainability* 7:15302-15318.

Ayawei, N., Ebelegi, A. N., and Wankasi, D. (2017). Isotherms-Review Article. *Hindawi Journal of Chemistry 2017*

Bankole, O. M., Oyeneyin, O. E., Olaseni, S. E., Akeremale, O. K.. and Adanigbo, P. (2019). Kinetics and Thermodynamic Studies for Rhodamine B Dye Removal Onto Graphene Oxide Nanosheets in Simulated Wastewater. *American Journal of Applied Chemistry* 7(1):10-24.

Essomba, J. S., Nsami, J. N., Belibi, P. D. B., Tagne, G. M. and Mbadcam, J. K. (2014). Adsorption of Cadmium(II) Ions from Aqueous Solution onto Kaolinite and Metakaolinite. *Pure and Applied Chemical Sciences* 2(1):11 – 30.

Fu, F. and Wang, Q. (2011). Removal of Heavy Metal Ions from Wastewaters: A Review. *Journal of Environmental Management* 92:407-418

Ghasemi, M., Mashhadi, S., and Azimi-Amin, J. (2018). Fe_3O_4/AC Nanocomposite as a Novel Nano Adsorbent for Effective Removal of Cationic Dye: Process Optimization Based on Taguchi Design Method, Kinetics, Equilibrium and Thermodynamics. *Journal of Water Environment and Nanotechnology* **3**(4):321-336.

He, Y, Wu, P, Xiao, W, Li, G., Yi, J. and He, Y. (2019). Efficient Removal of Pb(II) from Aqueous Solution by a Novel Ion Imprinted Magnetic Biosorbent: Adsorption Kinetics and Mechanisms. *Plos ONE* 14(3): E0213377. Journal.Pone.0213377

Hossain, M.A., Hao, N., Guo, H.W.S. and Nguyen, T.V. (2012). Removal of Copper from Water by Adsorption onto Banana Peels as Bioadsorbent. *International Journal of Geomaterial* 2:227-234

Hossain, M. A., Hossain, Md. L. and Tanim-al-Hassan (2016). Equilibrium, Thermodynamic and Mechanism Studies of Malachite Green Adsorption on Used Black Tea Leaves from Acidic Solution. *International Letters of Chemistry, Physics and Astronomy.* 64:77-88

Iakovleva, E. and Sillanpää, M. (2013). The Use of Low Cost Adsorbents for Wastewater Purification In Mining Industries. *Environmental Science and Pollution Research* 20(11):7878-7899.

Igwe, J.C and Abia, A.A. (2007). Adsorption Isotherm Studies of Cd (II), Pb(II) and Zn(II) Ions Bioremediation from Aqueous Solution Using Unmodified and EDTA-Modified Maize Cob. *Ecletica Química, São Paulo,* 32(1): 33-42.

Inyinbor, A. A., Adekola, F. A., and Olatunji, G. A.(2016). Liquid Phase Adsorptions of Rhodamine B Dye Onto Raw and Chitosan Supported Mesoporous Adsorbents: Isotherms And Kinetics Studies. *Applied Water Science* 7(5):2297-2307.

Inyinbor, A. A., Adekola, F. A. and Olatunji, G. A. (2015). Adsorption of Rhodamine B Dye from Aqueous Solution on *Irvingia Gabonensis* Biomass: Kinetics And Thermodynamics Studies. *South African Journal of Chemistry* 68:115–125.

Kampalanonwat, P. and Supaphol, P. (2014). The Study of Competitive Adsorption of Heavy Metal Ions from Aqueous Solution by Aminated Polyacrylonitrile Nanofiber Materials. *11th Eco-Energy and Materials Science and Engineering (11th EMSES). Energy Procedia* 56:142 – 151.

Kumar, R., Mudhoo, A., Lofrano, G. and Chandra, M. (2014). Biomass-Derived Biosorbents for Metal Ions

Online ISSN: 2736-0903
Print ISSN: 2736-089X
www.slujst.edu.ng

Sequestration: Adsorbent Modification and Activation Methods and Adsorbent Regeneration. *Journal of Environmental Chemical Engineering*. 2:239-259

Lakherwal, D. (2014). Adsorption of Heavy Metals: A Review. *International Journal of Environmental Research and Development* 4(1):41-48

Lasheen, M.R., Iman, Y. E., Shaimaa, T. E., Dina, Y. S. and El-Shahat, M.F. (2017). Heavy Metals Removal from Aqueous Solution Using Magnetite Dowex 50WX4 Resin Nanocomposite. *Journal of Materials and Environmental Sciences* 8(2): 503-511.

Lim, W., Kim, S. W., Lee, C., Choi, E., Oh, M. H., Seo, S. N., Park H. and Hamm S.(2019). Performance of Composite Mineral Adsorbents for Removing Cu, Cd, and Pb Ions from Polluted Water. *Scientific Reports 9:13598.*

Moftakhar, M. K., Yaftian, M. R. and Ghorbanloo, M. (2016). Adsorption Efficiency,Thermodynamics and Kinetics of SchiffBase-Modified Nanoparticles for Removal of Heavy Metals. *International Journal of Environtal Science and Technology.*13:1707–1722

Miretzky, P., Saralegui, A., and Cirelli, A. F. (2006). Simultanoeus Heavy Metal Removal Mechanism by Dead Macrophytes. *Journal of Chemosphere* 62:247- 254

Onwu, F.K and Ngele, S.O. (2015). Equilibrium and Thermodynamic Studies on Adsorption of Cd^{2+} and Zn^{2+} Using *Brachystegia Eurycoma* Seed Coat as Biosorbent. *Research Journal of Chemical Sciences* 5(2):32-41.

Rasheed, A., Farooq, F. and Rafique, U. (2013). Kinetics Study of Metal Removal Using Apple Peels: Closed Batch Approximation Model. *International Journal of Chemical and Environmental Engineering* 4(5): 281-285

Sarı, A. and Tuzen, M. (2009). Kinetic and Equilibrium Studies of Biosorption of Pb(II) and Cd(II) from Aqueous Solution by Macrofungus (*Amanita Rubescens*) Biomass. *Journal of Hazardous Materials* 164:1004–1011.

Singh, N. and Gupta, S. K. (2016). Adsorption of heavy metals: A review. *International Journal of Innovative Research in Science, Engineering and Technology* 5(2):2267- 2281.

Tie, J., Fang, X., Wang, X., Zhang, Y., Gu, T., Deng, S., Li, G., and Tang, D. (2017). AdsorptiveRemoval of a Reactive Azo Dye Using Polyaniline-Intercalated Bentonite. *Polish Journal of Environmental Studies* 26(3):1259-1268.

Worch, E. (2012). Adsorption Technology in Water Treatment: Fundamentals, Processes, and Modelling. Published by Berlin, Walter de Gruyter.

Yildiz, S. (2017). Kinetic and Isotherm Analysis of Cu(II) Adsorption onto Almond Shell (*PrunusDulcis*). *Ecological Chemistry and Engineering S.* 24(1):87-106.

